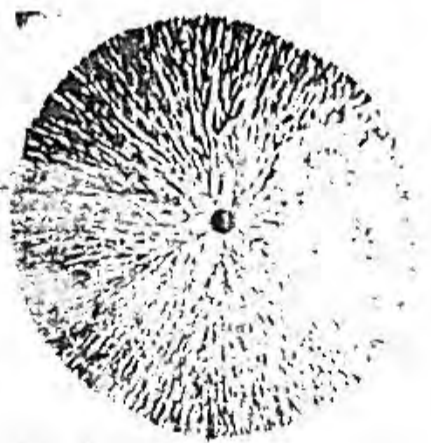
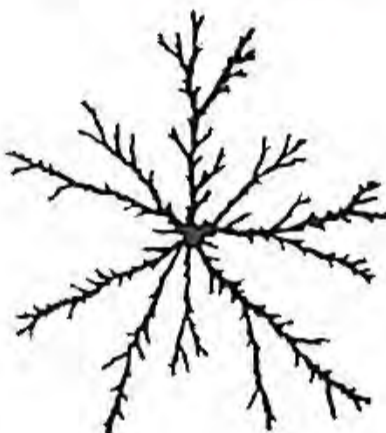
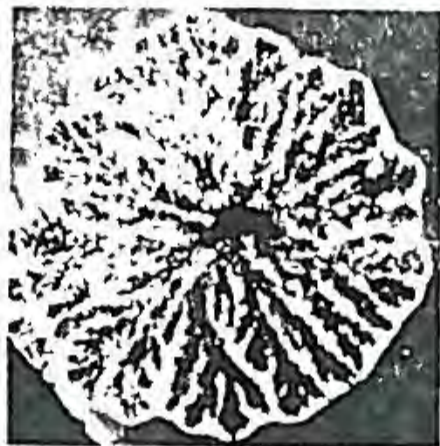


# Fractal Growth Phenomena

Tamás Vicsek

*Institute for Technical Physics  
Budapest, Hungary*



WORLD SCIENTIFIC  
Singapore

Scaling, non-analytic, critical exponents, critical point universality  
 $C(r) \sim Ar^\alpha$   $r \rightarrow br$   $C(br) \sim D r^\alpha$   
 $D = A \cdot b^\alpha$

PART II.  
CLUSTER GROWTH  
MODELS

*Chapter 5.***LOCAL GROWTH MODELS**

In Part II. models based on growing structures made of identical particles will be treated. While in Chapter 2. mostly artificial examples were discussed, here we shall concentrate on more realistic models which are constructed in order to reflect the essential features of specific growth phenomena occurring in nature. Various models allowing exact or numerical treatment have been playing an important role in the studies of growth. Because of the complexity of the phenomena it is usually a difficult task to decide which of the factors affecting the growth plays a relevant role in determining the structure of the growing object. In a real system the number of such factors can be relatively large, and this number is decreased to a few by appropriate model systems. Thus, the investigation of these models provides a possibility to detect the most relevant factors, and demonstrate their effects in the absence of any disturbance.

Structures consisting of connected particles are usually called *clusters* or *aggregates*. In most of the cases the growth will be assumed to take place on a *lattice* for computational convenience, and two particles are regarded as connected if they occupy nearest neighbour sites of the lattice. However, for studying universality and related questions, *off-lattice* or further neighbour versions of clustering processes can also be investigated. A lattice site with a particle assigned to it is called occupied or filled. An important additional

feature included into the majority of models to be described is stochasticity which is typical for growth phenomena.

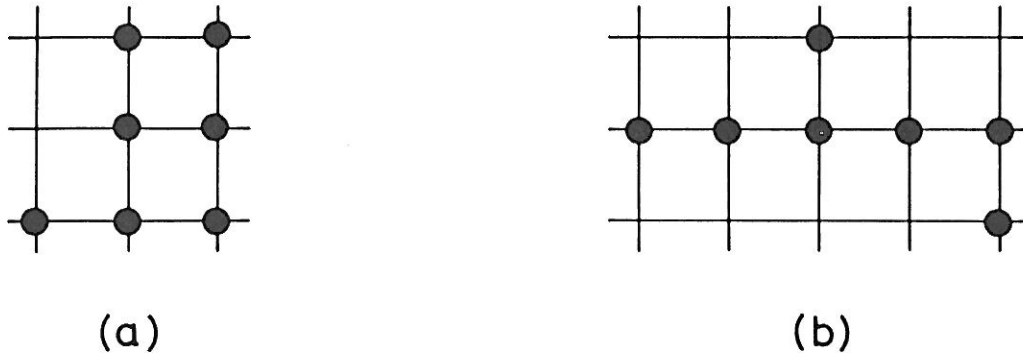


**Figure 5.1.** Two possible configurations (clusters) consisting of the same number of particles (black sites). The statistical weight of a given cluster depends on its geometry. For example, the probability associated with configuration (a) is larger for a growth process which preferably produces compact clusters.

In general, a stochastic cluster growth model may lead to all possible configurations which can be formed from a given number of particles. What makes these models differ from each other is the weight or probability  $P_{N,i}$  associated with a given configuration  $i$  consisting of  $N$  units (Fig. 5.1).  $P_{N,i}$  can be different for the same configuration even in the same model, because generally it depends on the sequence, according to which the individual particles are added to the cluster (Herrmann 1986). The distribution of  $P_{N,i}$  as a function of  $i$  is uniquely related to the particular model investigated, and determines the value of the quantity

$$S_N(q) = -\frac{1}{N(q-1)} \ln \sum_i P_{N,i}^q \quad (5.1)$$

analogous to the order  $q$  Rényi information. On the basis of (5.1) it is possible to define (Vicsek *et al* 1986)

$$S = \lim_{q \rightarrow 1} \lim_{N \rightarrow \infty} S_N(q) = - \lim_{N \rightarrow \infty} \frac{1}{N} \sum_i P_{N,i} \ln P_{N,i}. \quad (5.2)$$

corresponding to the configurational entropy of a given cluster growth model.

In the following we shall distinguish two main types of cluster growth processes, depending on the global character of the rule which is used in the course of adding a particle (or a cluster of particles) to the growing cluster. *The rule will be called local if it depends only on the immediate environment of the position where the new particle is to be added.* In other words, when deciding whether to add a particle at site  $\vec{x}$  only the status (filled or not) of the nearest or next nearest neighbours of this site is taken into account. On the contrary, *in non-local models the structure of the whole cluster can affect the probability of adding a site at a given position.*

### 5.1. SPREADING PERCOLATION

In this Section we shall consider a model which represents perhaps the simplest growth process leading to a branching fractal structure (Leath 1976, Alexandrowitz 1980). The process starts with a single seed particle placed onto a site of a lattice. Its neighbouring sites are considered live in the sense that they potentially may become occupied in the future. Next, one of these live sites is chosen randomly and (i) filled with a particle with a probability  $p$  or (ii) killed for the rest of time with a probability  $1 - p$ . Occupation of a site with probability  $p$  is realized by generating a random number  $r$  (with a uniform distribution on  $[0, 1]$ ) and filling the site if  $r < p$ . The filled site becomes part of the growing cluster and its new neighbours become living sites. A large cluster is grown by repeating the same procedure many times. In a variation of this model at each time step all of the living or *growth sites* are considered for occupation, instead of one at a time, therefore, the cluster grows by adding shells to it. In addition, one can replace the seed particle with a hyperplane of seed particles.

The above process is relevant to a number of spreading phenomena, including epidemics, chemical reactions, flame propagation, etc. For example, using the language of epidemic, the live sites are susceptible to infection, the killed sites are immune, while the occupied sites correspond to infected individuals (Grassberger 1983). An epidemics will spread over the whole population if there is always at least one live site. Fig. 5.2 shows a configuration of filled sites generated on a triangular lattice using a straight interval

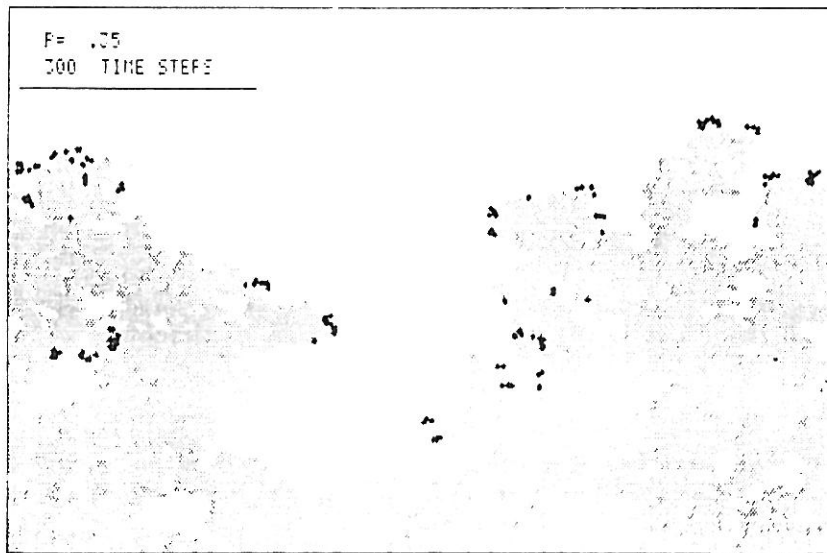


**Figure 5.2.** Result of a typical run of growing a percolation cluster along a line for  $p = p_c$ . The cluster is generated on a triangular lattice by adding to it all of the growth sites at each time step. The growth sites are denoted by heavy dots. (Grassberger 1985).

as the seed configuration. It seems to have a complex structure with holes and fjords having no characteristic size that is typical for fractal clusters.

Note, that although the random numbers  $r$  are generated during the growth, the same configurations are obtained as if we had assigned to all of the sites of the lattice a random number previously, then defined equilibrium percolation clusters as connected objects consisting of sites for which  $r < p$  and started the process afterwards. Therefore, the above model is equivalent to a simple type of growth on a static percolation cluster and as the available sites of a given configuration are filled we gradually recover an equilibrium percolation cluster. The growth stops when all sites belonging to the cluster containing the seed particle are filled. Starting the spreading algorithm many times with different initial conditions one can reproduce ordinary percolation clusters with a size distribution corresponding to  $p$ .

Equilibrium percolation is a widely used model for describing various properties of inhomogeneous media (Stauffer 1985). Here we only recall those results of percolation theory which are related to the fractal nature (Stanley 1977) of spreading percolation clusters. In particular, when  $p$  is increased,

at  $p = p_c$  a transition takes place which is manifested in the appearance of a connected infinite cluster having a density for  $0 < p - p_c \ll 1$

$$P(p) \sim (p - p_c)^\beta, \quad (5.3)$$

where  $\beta > 0$  is the critical exponent of the percolation probability,  $P(p)$  and  $p_c$  is called percolation threshold. In the following we consider the properties of the infinite cluster. The correlation length diverges at  $p_c$  according to

$$\xi \sim |p - p_c|^{-\nu_p} \quad (5.4)$$

where  $\xi$  corresponds to the radius at which the power law decay of the pair correlation function  $c(r)$  (see (2.14)) crosses over into a constant behaviour. As before, because of scaling we can assume that for  $\xi \gg a$  and  $r \gg a$  ( $a$  is the lattice spacing) the only relevant length is  $\xi$ , and correspondingly (Kapitulnik *et al* 1985),

$$c(r) \sim P(p)f(r/\xi), \quad (5.5)$$

where the scaling function  $f(x)$  approaches a constant for  $x \rightarrow \infty$ . For  $x \ll 1$  we expect that  $c(r)$  is independent of  $\xi$  which can be satisfied only if  $f(x) \sim x^{-\beta/\nu_p}$  for  $x \ll 1$ . From here and using (5.3) and (5.4) we find  $c(r) \sim r^{-\beta/\nu_p}$  for  $r \ll \xi$ . Then, in analogy with the arguments leading to (2.18) one obtains for the fractal dimension of the infinite cluster at  $p_c$  ( $\xi \rightarrow \infty$ )

$$D = d - \frac{\beta}{\nu_p}. \quad (5.6)$$

The exponents  $\beta$  and  $\nu_p$  are known exactly for  $d = 2$  and can be calculated by numerical or theoretical methods for higher dimensions. For example, in two dimensions  $\nu_p = \frac{4}{3}$  and  $\beta = \frac{5}{36}$  gives for the fractal dimension of the infinite cluster at  $p_c$   $D = \frac{91}{48} \simeq 1.896$ .

As mentioned above the spreading percolation process reproduces a

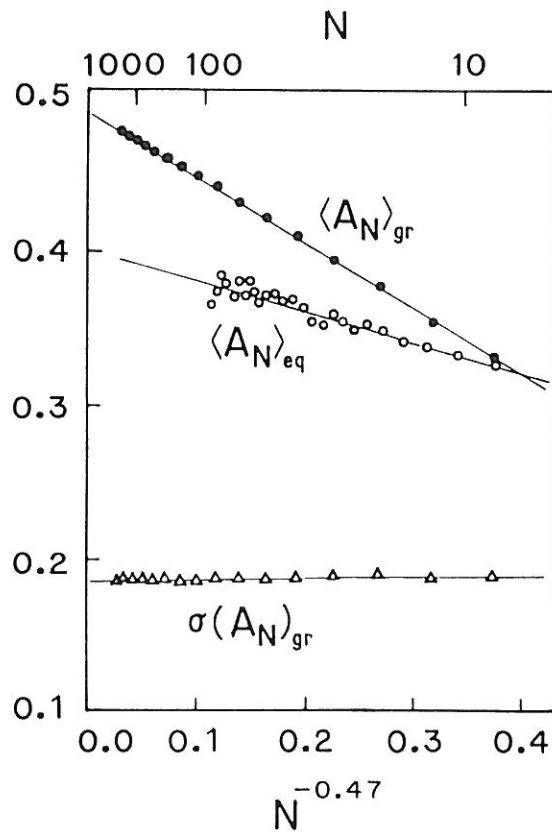


**Figure 5.3.** The average anisotropy of equilibrium ( $\langle A_N \rangle_{eq}$ ) and growing ( $\langle A_N \rangle_{gr}$ ) percolation clusters as a function of  $N^{-\theta}$ , where  $\theta = 0.47$  is the correction-to-scaling exponent. The fluctuation in the anisotropy of growing percolation clusters,  $\sigma(A_N)_{gr}$ , is also shown (Family *et al* 1985).

static percolation cluster, when it terminates. However, if the growth on the given finite cluster is not completed yet, the structure of the growing and equilibrium percolation clusters is not exactly the same. According to the simulations the fractal dimension determined during the growth is not affected by the algorithm, but the same is not true for the overall shape of the clusters (Family *et al* 1985). This can be shown by calculating the radius of gyration tensor and determining the ratio,  $\langle A_N \rangle$ , of the principal radii of gyration. The results presented in Fig. 5.3 demonstrate that spreading percolation clusters are in the asymptotic limit elongated, but to a smaller extent than the static ones.

The truly *dynamic behaviour* of growing percolation clusters can be interpreted in terms of the total number and distribution of *growth sites*



which are here defined as filled sites having live neighbours. Let us first consider spreading at  $p = p_c$  occupying one site at each time step. The total number of growth sites  $N_G$  scales with the number of particles in the cluster  $N$  as (Family and Vicsek 1985, Herrmann and Stanley 1985)

$$N_G \sim N^\delta, \quad (5.7)$$

where  $N$  plays the role of time. Since the radius of the region over which the growth sites are scattered increases as  $N^{1/D}$ , we conclude that the set of growth sites forms a fractal of dimension  $D_G = \delta D$ . In the case of filling shells (considering all live sites simultaneously for occupation) at a given time step  $t$ , one has a different law (Alexandrowitz 1980)

$$N_G(t) \sim t^{d_s-1}, \quad (5.8)$$

where  $d_s$  is called the spreading or chemical dimension. Comparing (5.7) and (5.8) one gets

$$\delta = \frac{d_s - 1}{d_s}. \quad (5.9)$$

Introducing the exponent  $\nu_{||}$  through the relation  $R(t) \sim t^{\nu_p/\nu_{||}}$ , where  $R(t)$  is the average radius of the infected region, it is possible to derive an additional relation (Grassberger 1983, 1985) involving the exponents already defined

$$d_s = \frac{2\nu_p - \beta}{\nu_{||}}. \quad (5.10)$$

Both (5.9) and (5.10) are supported by numerical simulations (Herrmann and Stanley 1985, Grassberger 1985). For  $d = 2$  the following results were obtained:  $\delta \simeq 0.402$ ,  $d_s \simeq 1.675$  and  $\nu_{||} \simeq 1.509$ .

A more detailed description of the dynamics of spreading is provided by the radial distribution of growth sites  $N_g(r, N)$ , where  $N_g(r, N)\Delta r$  is the number of growth sites located from the seed at a distance between  $r$

and  $r + \Delta r$  and  $N$  is the actual number of already occupied sites. Scaling considerations suggest, and related simulations support that (Herrmann and Stanley 1985)

$$N_g(r, N) \sim N^{\delta-1/D} f\left(\frac{r}{N^{1/D}}\right). \quad (5.11)$$

This scaling form expresses the fact that the distribution is determined by only one relevant length scale proportional to  $R \sim N^{1/D}$ . The prefactor  $N^{\delta-1/D}$  is included to satisfy  $\int N_g(r, N) dr \sim N^\delta$  (see Eq. (5.7)). Here and in the following the scaling behaviour of such integrals is determined by performing a change of variable  $z = r/N^{1/D}$ .

Similarly, one can determine the function  $P(r, N)$  which is the probability of choosing a growth site being at a distance  $r$  from the seed after  $N$  particles have been added to the cluster. Again, the only relevant parameter is  $N$  and (Bunde *et al* 1985a)

$$P(r, N) \sim N^{-1/D} g\left(\frac{r}{N^{1/D}}\right), \quad (5.12)$$

where the scaling function  $g(x)$  typically is close to a Gaussian. Scaling laws like (5.11) or (5.12) can be checked numerically by collecting data for various  $r$  values and examining whether the results fall onto a universal curve when plotting the appropriately rescaled variables.

The problem of spreading percolation has attracted considerable interest recently. It was analysed by field theoretical formalism (Cardy and Grassberger 1985), modified by i) taking into account revival of the dead sites (Ohtsuki and Keyes 1986) and by ii) introducing various rules for choosing a growth site before making a decision about filling one (e.g. Bunde *et al* 1985b).

## 5.2. INVASION PERCOLATION

Invasion percolation was introduced in order to simulate the *displacement of one fluid by another in porous media* under the condition that the capillary forces dominate the motion of the interface (Lenormand and Bories 1980, Chandler *et al* 1982). Many porous media may be represented conveniently as a network of pores joined by narrower connecting throats. Consider the process of a non-wetting fluid, say oil, being displaced from such a medium by a wetting fluid, say water, at a constant but very small flow rate. In this limit the capillary forces dominate which are the strongest at the narrowest places in the medium. The interface moves quickly through a throat but gets stuck in the larger pores. This motion can be represented as a series of discrete jumps in which at each time step the water displaces oil from the smallest available pore.

As the water behind the interface advances, it may entirely surround regions filled with oil. Since oil is incompressible, one must take into account in a model that water can not invade finite, isolated regions of "residual oil".

The model for computer simulation of the above process is defined on a lattice. i) A random number drawn from the uniform distribution on the unit interval is assigned to each site of a cell of linear size  $L$ . ii) As in the growing percolation model the process starts with a seed particle or a surface and goes on by subsequent occupation of one of the perimeter sites (empty sites which are nearest neighbours of the cluster). iii) However, the perimeter site to be occupied is not selected randomly, but the one with the smallest random number  $r$  (corresponding to the smallest capillary force) is occupied.

In this version of the invasion percolation model (which simulates the interface motion, if one of the fluids is infinitely compressible) the process does not stop until the finite cell is filled in completely, since we do not have a temperature like parameter analogous to the occupation probability  $p$  of ordinary percolation. On the other hand, as a well defined configuration one can study the structure of the region filled in by the invader fluid at the point in time when the invader first percolates, i.e., first forms a connected

path between the two opposite edges of the cell. According to the simulations (Wilkinson and Willemsen 1983) the number of sites occupied by the invader at this moment can be expressed as  $N \sim L^D$ , where  $D \simeq 1.89$  in two and  $D \simeq 2.52$  in three dimensions. These values for the fractal dimension of the invasion percolation clusters are in good agreement with those obtained for the ordinary percolation clusters, showing the similarity between the static properties of the two models.

To take into account the incompressibility of the fluids one needs an additional rule: Once a region filled by “defender” sites has been surrounded by the invading fluid none of the sites belonging to this “trapped” area is available for occupation by the invading fluid. In this case the fractal dimension of the cluster which is made of the invaded sites at the moment the invader first percolates the two dimensional cell was found to be  $D \simeq 1.82$  (Chandler et al 1982). This value is different from  $D \simeq 1.89$  and indicates that invasion percolation with trapping and ordinary percolation belong to distinct universality classes.

One way to quantify the difference between static and invasion percolation is to investigate the cumulative acceptance profile  $a_N(r)$  defined by (Wilkinson and Willemsen 1983)

$$a_N(r) = \frac{\langle \text{no of random numbers in } [r, r + dr] \text{ accepted into cluster} \rangle_N}{\langle \text{no of random numbers in } [r, r + dr] \text{ considered} \rangle_N}. \quad (5.13)$$

It can be shown that asymptotically

$$a_\infty = \begin{cases} 1 & \text{if } r < p_c, \\ 0 & \text{if } r > p_c. \end{cases} \quad (5.14)$$

This is the same as the acceptance profile of static percolation, which is valid in the present case only in the large  $N$  limit. Furthermore, for invasion percolation with trapping (5.14) *breaks down* and  $a_N(r)$  does not approach a step function.

There is an additional threshold in the trapping version of invasion

percolation in  $d > 2$ . It takes place when the largest, originally spanning region of invader free (defender) sites breaks into finite isolated clusters. At this point further deviations from the ordinary percolation behaviour can be observed. The finite but large clusters of defender sites can be considered as fractals. Their fractal dimension in  $d = 3$  was found to be  $D_{def} \simeq 2.13$  which is different from both  $D$  of the invaded region and  $D$  of the ordinary percolation clusters.

In an analogy with static percolation one can define the defender cluster size distribution  $n_s$  as the normalized number of clusters consisting of  $s$  defender particles. The simulation results support the scaling assumption (Willemsen 1984)

$$n_s \sim n_0(L) s^{-\tau} \quad (5.15)$$

with  $\tau \simeq 2.07$  in three and  $\tau < 2$  in two dimensions. This  $\tau$  does not satisfy the relation  $\tau = 1 + d/D$  known from static percolation. Instead, in  $d = 3$

$$\tau = 1 + \frac{d'}{D_{def}} \quad (5.16)$$

holds with  $d' \simeq 2.24$ . An important consequence of (5.16) is that  $n_0(L)$  should scale with  $L$ . This is even more explicitly manifested in two dimensions, because of  $\tau < 2$ .

At first sight the latter result is surprising since  $\tau > 2$  is a condition which can be derived for ordinary percolation from mass conservation (the sum  $\sum_s s n_s$  must converge as  $s \rightarrow \infty$ ). However, the set of isolated defender regions at the threshold can be associated with the so called volatile fractals (Herrmann and Stanley 1984) for which  $\tau < 2$  has been shown to be the consistent value (Vicsek and Family 1984, Herrmann and Stanley 1984). In the present case mass conservation with  $\tau < 2$  is provided by the  $L$  dependence of the prefactor  $n_0(L)$  which should decay with growing  $L$  compensating the divergence of the above sum.

This behaviour can be interpreted by the following mechanism. As

one goes to a larger cell, some of the smaller isolated clusters may turn out to be connected through parts which were outside of the original cell, and form larger clusters. Consequently, when  $L$  increases, there is a net decrease in the density of clusters of a given size. In general, the condition for the scaling of  $n_0(L)$  is  $d' < d$ .

### 5.3. KINETIC GELATION

The term gelation is generally used for a transition when some of the finite clusters in the system join to form a single large cluster spanning the whole sample. This phenomenon is accompanied by relatively drastic changes in the physical properties of the system, e.g., its shear viscosity sharply increases. The clusters can be made of many kinds of particles ranging from molecules to red blood cells.

In the following we shall use the language of sol-gel transition which takes place in a liquid mixture of sol molecules and neutral solvent molecules under specific conditions. Originally the sol molecules are separated and are called monomers. With time the monomers form chemical bonds with each other producing dimers, trimers and so on. During this irreversible process the mean cluster size gradually increases, and at a given moment,  $t_g$ , called gelation time, the linear size of the largest molecule becomes equal to that of the system. This single spanning cluster is called gel and its weight grows further after  $t_g$ . Its mass represents only a small percentage of the mass of all sol and solvent molecules which are typically trapped in the holes formed by the gel, thus the sample behaves as a soft but elastic material (gelatine). The gelation process is largely influenced by the maximum number of chemical bonds  $f$  (functionality) associated with a monomer, for example, molecules with  $f = 2$  do not contribute to the sol-gel transition.

Depending on the mechanism by which two molecules can form a chemical bond various models can be used to describe gelation. In polycondensation a bond appears suddenly as a result of either i) an external excitation or ii) the collision of molecules. In the first case the motion of the molecules can be neglected and static percolation can be used to characterize

the phenomenon. In the other limit, when it is exclusively the diffusion of clusters which determines the bond formation rate, diffusion-limited cluster-cluster aggregation (to be discussed in Chapter 8.) is a good candidate for an appropriate model.

The kinetic gelation model was introduced to simulate another type of gelation called *addition polymerization*. In this process unsaturated electrons jump from one molecule to the other, meanwhile assisting in producing bonds. As an important deviation from static percolation in this case the bonds are strongly correlated in space. Generally, one assumes that the mobility of sol molecules is much smaller than that of the electrons.

Let us consider the following *lattice model* of the above process (Manneville and de Seze 1981). i) Monomers are placed randomly at the sites of a cell of linear size  $L$  and periodic boundary conditions are imposed. Empty sites are solvents with functionality  $f = 0$  and have a concentration  $1 - \sum_i c_i$ , where  $c_i$  is the concentration of monomers of functionality  $f = i$ . ii) Initiators (radicals) are randomly added to sites with a monomer already sitting on them. The concentration of initiations is usually chosen to satisfy the condition  $c_I = c_I(t = 0) \ll 1$ . iii) At each growth step one of the radicals is randomly selected. Next, the radical attempts a jump in a random direction along one of the bonds leading out from the site. Such a transfer is prohibited if the site at the other end of the bond has zero functionality. The time is increased by an amount  $\delta t = [c_I(t)L^d]^{-1}$  even if the attempt fails. iv) After a successful jump the functionality of the sites connected by the given bond is decreased by one and the bond becomes occupied. v) If a radical happens to be at the new site, the two radicals annihilate, thus  $c_I(t)$  is slowly decreasing in time. A radical can also get trapped in a site which has no nearest neighbour sites of functionality larger than zero. In a finite cell all of the radicals become trapped within a finite time.

This extensive list of rules can be programmed relatively easily and the resulting configurations are evaluated in terms of quantities analogous to those used in static percolation. A cluster is defined as a set of sites which can be connected through occupied bonds. The actual status of the gelation process is characterized by the cluster size distribution function  $n_s(t) =$

$L^{-d}N_s(t)$ , where  $N_s(t)$  is the number of clusters consisting of  $s$  monomers at time  $t$ . The concentration of occupied bonds,  $p$ , increases monotonically with  $t$  and can be used to monitor the development of gelation with a sol-gel transition taking place at  $p_c$ .

Large scale Monte Carlo simulations of three-dimensional kinetic gelation (Herrmann *et al* 1982) have shown that the critical exponents  $\beta$  and  $\nu_p$  defined in (5.3) and (5.4) within the errors are the same for this process as for ordinary percolation. Consequently, the fractal dimension  $D = d - \beta/\nu_p$  of the spanning gel molecule also coincides with the fractal dimension of the infinite static percolation cluster at  $p_c$ .

This universal behaviour of the two models seems to *break down* when one studies the quantity  $A$  which is the *ratio of the critical amplitudes* of the second moment of  $n_s$

$$\chi_{q=2} = \sum_{s < \infty} s^2 n_s \sim \begin{cases} a^+ (p - p_c)^{-\gamma}, & \text{if } p \rightarrow p_c^+ \\ a^- (p_c - p)^{-\gamma}, & \text{if } p \rightarrow p_c^- \end{cases} \quad (5.17)$$

Here  $\gamma$  is another critical exponent and  $a^+$  and  $a^-$  are the amplitudes, so that  $A = a^-/a^+$ . The cluster size distribution in systems exhibiting critical behaviour generally scales with  $s$  and  $p - p_c$  as (Stauffer 1985)

$$n_s \sim s^{-\tau} f(|p - p_c|s^\sigma), \quad (5.18)$$

where  $\tau$  and  $\sigma$  are further critical exponents connected to the previously introduced exponents through scaling relations, and  $f(x)$  is a scaling function. In the theory of equilibrium critical phenomena it is assumed that  $f(x) = BF(Cx)$ , where  $B$  and  $C$  are constants which may depend on the properties of the system investigated, but  $F(x)$  is supposed to be universal, i.e., the same for all systems belonging to a relatively broad class. This assumption together with (5.17) and (5.18) leads to the conclusion that  $A$ , the ratio of  $a^+$  and  $a^-$ , has to be universal. According to the numerical simulations of three-dimensional percolation  $A \simeq 10$ .

A careful analysis of the amplitude ratio  $A$  for kinetic gelation in  $d = 3$



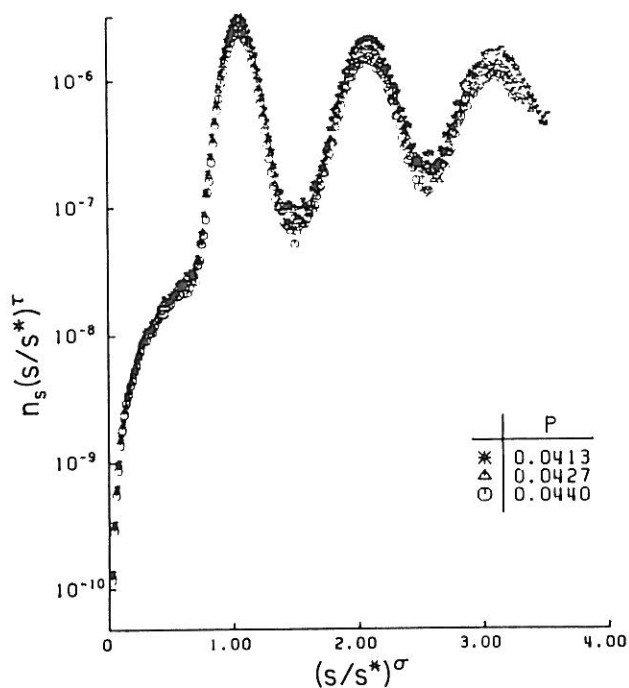


**Figure 5.4.** Scaling plot of the data for the cluster-size distribution in three-dimensional kinetic gelation. The data are for  $L = 60$  and  $c_I = 0.0003$  (Chhabra *et al* 1984).

(Herrmann *et al* 1982) showed that it is generally considerably smaller than 10. In fact, it decreases with the initial concentration of radicals  $c_I$ , and in the limit  $c_I \rightarrow 0$  tends to become equal to 1. This means that  $F(x)$  has to be different from that describing the scaling in ordinary percolation, therefore, the two models *belong to different universality classes*. An interesting observation was recently made concerning  $A$  in a system with regularly distributed initiators, where  $A$  was found to be approximately equal to 10 (Herrmann 1986). This result suggests that the randomness of the positions of initiators is essential, in apparent analogy with the problem of diffusion in a medium with randomly or regularly distributed traps and (continuum) percolation of overlapping spheres (Balberg 1987).

An additional sign of non-universality of kinetic gelation is manifested in the behaviour of  $n_s$ . Although the scaling assumption (5.18) for the cluster size distribution function is known to describe  $n_s$  adequately in many different systems, it is not consistent with the data obtained for kinetic gelation. Instead, it shows oscillations of period  $s^* \simeq p/c_I$ , and scales as (Chhabra *et*

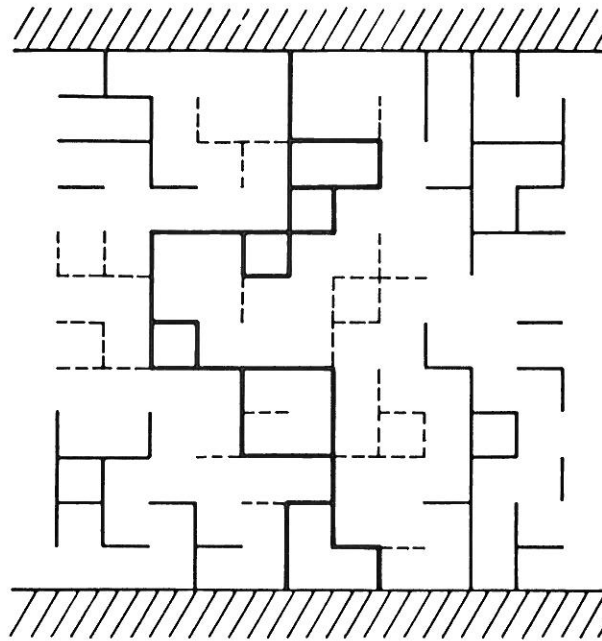


**Figure 5.5.** Schematic picture of the backbone of a percolation cluster. The bonds belonging to the backbone are drawn with heavy lines, while the bonds leading to dead ends are denoted by dashed lines.

al 1984)

$$n_s \sim \tilde{s}^{-\tau} e^{-b|p-p_c|\tilde{s}^\sigma} f(\tilde{s}) e^{c(p-p_c)}, \quad (5.19)$$

where  $b$  and  $c$  are constants and  $\tilde{s} = s/s^*$ . Fig. (5.4) shows the scaling function  $f(x)$  determined from numerical simulations and using (5.19). Note, that if  $f(x)$  tends to a constant value for large  $x$ , the last two terms represent only a correction to the original scaling form. This, however, does not seem to be the case, since for  $c_I \rightarrow 0$  the oscillations are not found to be damped entirely.

Returning to the structure of the gel molecule at  $p_c$  we recall that it is a fractal having a dimension equal (or close) to  $D$  of the infinite cluster in static percolation at  $p_c$ . In addition to its dimension a fractal can be characterized by other quantities related to its internal structure. For example, in Chapter 3. it has been shown that a singular distribution on a fractal defines an infinite number of subsets all having a fractal dimension smaller or equal

to  $D$ . One of the simplest subsets of a fractal is its “backbone” which can be introduced through the voltage distribution on a cluster (see Example 3.2). Consider now a large cluster of resistors with two electrodes – one at each of its opposite edges. Then the backbone is defined as the set of bonds (resistors) with a voltage drop different from zero. It is easy to see that  $D_{BB} = D_0$ , where  $D_{BB}$  is the dimension of the backbone and  $D_0$  is the generalized dimension corresponding to the zero-th moment of the voltage distribution. According to an equivalent definition of backbone, it is a set of bonds (sites) which can be connected staying on the fractal to both electrodes via at least two routes having no overlaps. In short, routes leading to dead ends are thrown away and only relevant loops contribute to the backbone (Fig. 5.5).

The fractal dimension of the backbone of a cluster is an independent exponent characterizing the “loopness” of the structure. For example, in three-dimensional static percolation  $D_{BB} \simeq 1.74 < D \simeq 2.5$ .  $D_{BB}$  has also been determined for kinetic gelation in  $d = 3$ . It was found to be approximately equal to 2.22 (Chhabra *et al* 1985), a value considerably larger than  $D_{BB}$  for percolation. This can be understood; the main contribution to the mass of the clusters comes from loops formed by chains generated by randomly walking radicals.

To take into account experimental realizations many variations of the kinetic gelation model have been considered, including simulations with poison sites disabling radicals (Pandey and Stauffer 1983) and mobile solvent molecules (Bansil *et al* 1984).

#### 5.4. RANDOM WALKS

Investigation of various types of random walks represents a particularly effective approach to the description of systems consisting of growing, non-branching objects (de Gennes 1979). The most important example is *polymerization*, where monomer molecules of functionality 2 (being able to form two chemical bonds) are joined together leading to a long chain called linear polymer molecule. In most of the cases walks on a lattice are considered,

the lattice sites corresponding to a monomer. The set of sites visited by the walker is regarded as a chain of molecules or particles (in general, multiple occupation of a site is allowed). For simplicity we shall use the term random walk for this trail.

In an actual realization, a random walk starts from an initial position and proceeds by making jumps of one lattice unit in a direction which is selected randomly from the directions allowed by the given model. For example, when strictly self-avoiding walks are considered, there is no allowed direction if all of the nearest neighbours of the current position of the walking particle are occupied, and the walk must terminate. In this section we shall concentrate on walks which are truly growing, i.e., are never trapped by themselves. Assuming that the particle makes one step in a unit interval, the number of steps in a walk  $N$  is equal to the duration of the walk,  $t$ .

The most fundamental quantity used for characterization of random walks is their *mean squared end-to-end distance*  $\langle R_e^2(t) \rangle = R_0^2(t)$ , where  $R_e(t)$  is the distance between the walking particle and the initial position at time  $t$ . It measures the square of the average spatial extent of a walk,  $R_0(t)$ , and its time dependence will allow us to make conclusions about the fractal nature of the process. In particular, if

$$R_0(t) \sim t^\nu \quad (5.20)$$

the quantity  $D = 1/\nu$  will be identified with the fractal dimension of the chain.

#### 5.4.1. Self-intersecting random walks

The simplest version of random walks is a sequence of jumps in random directions, where there is no constraint on the probability of jumping to any of the neighbouring sites. This process can also serve as a lattice model for diffusion, and we shall also refer to unrestricted random walks as trails of diffusing particles. As was briefly discussed in Example 2.6, the trail of a

diffusing particle has fractal properties. To see this let us denote the end-to-end vector at time  $t$  by  $\vec{R}_e(t) = \sum_{i=1}^t \vec{a}_i$ , where  $\vec{a}_i$  is a vector of length  $a$  equal to the lattice spacing and it has  $z$  possible orientation with  $z$  being the coordination number. Then

$$\langle R_e^2(t) \rangle = \sum_{i,j} \langle \vec{a}_i \vec{a}_j \rangle = a^2 t + 2 \sum_{i>j} \langle \vec{a}_i \vec{a}_j \rangle \sim t, \quad (5.21)$$

since due to the independence of the orientations of  $\vec{a}_i$ -s the cross products vanish. Accordingly, the characteristic linear size of a walk is  $R_0(t) \sim t^{1/2}$ . For a walk starting at  $t = 0$  it is also straightforward to show that the probability of finding the walker at a distance  $R$  from the origin is asymptotically  $P(R, t) \sim e^{-R^2/Dt}$ , where  $D = a^2/\Delta t$  with  $\Delta t = 1$  in our case.

Let us consider the set of sites which are visited by a walk of duration  $t$  at time intervals  $t \gg \Delta t' \gg 1$ . The typical distance of these sites is  $l \sim (\Delta t')^{1/2}$ , since the walks which take place during each time interval  $\Delta t'$  are themselves independent random walks. Consequently, the whole walk can be covered by  $N(l)$  boxes of linear size  $l$ , where

$$N(l) = \frac{t}{\Delta t'} \sim t l^{-2}. \quad (5.22)$$

This expression corresponds to the definition of fractal dimension with  $D = 2$ . In obtaining (5.22) we implicitly assumed that the random walks of size  $l$  do not overlap and we need a separate box to cover each of them. This is obviously not true in one dimension which is indicated by the fact that  $D > d$  in this case. The  $D = d = 2$  case is marginal, while in  $d > 2$  the fraction of overlaps becomes negligible and a true self-similar object is generated by random walks. Note, however, that one can consider the number of steps  $t$  made within a region of radius  $R_0$ , instead of the number of distinct sites visited by the walker. Then regarding  $t$  as the number of particles within this region the scaling of mass  $M(R_0) \sim R_0^2$  has the same form as (5.22) even in  $d < 2$ . Fig. 2.10 shows a long random walk on the plane together with its external perimeter.

The situation does not change qualitatively if the jump direction depends merely on a finite number of previously completed steps. Let us suppose that only the last  $\Delta t'$  steps affect the probability to jump in a given direction. In the next step this probability has to be strictly independent of the history preceding the last  $\Delta t'$  steps. Then one can define a walk which is made of sites visited at times separated by a time interval larger than  $\Delta t'$  and the previously considered model is recovered. Therefore, finite time memory has no effect on the asymptotic behaviour.

The *overall shape* of unrestricted random walks is asymptotically highly *anisotropic*. Numerical simulation shows that the ratios of the squared principal radii of gyration of three dimensional walks are the following (Solc 1973)

$$\langle R_1^2 \rangle : \langle R_2^2 \rangle : \langle R_3^2 \rangle = 11.8 : 2.69 : 1.00. \quad (5.23)$$

There is an exact result for the quantity

$$A_d = \frac{\sum_{i>j}^d \langle (R_i^2 - R_j^2)^2 \rangle}{(d-1) \langle \left( \sum_{i=1}^d R_i^2 \right)^2 \rangle}, \quad (5.24)$$

measuring the asphericity of a walk in  $d$  dimensions. Here  $R_i^2$  is the square of the  $i$ th principal radius of a walk (the  $i$ th eigenvalue of the corresponding radius of gyration tensor). According to the analytical calculations (Rudnick and Gaspary 1986)

$$A_d = \frac{2(d+2)}{(5d+4)} \quad (5.25).$$

There are several ways to modify the above discussed simplest case. If the direction of each step is correlated by the direction of the previous one, the situation changes qualitatively. In this case arbitrarily distant points also become correlated, and the mean square distance diverges according to an exponent  $R_0^2(t) \sim t^{2H}$ , where  $H$  and the correlations are related (see Example

2.8). The fractal dimension corresponding to the set of points visited by a walker for a given  $H$  is

$$D = \frac{1}{H} \quad (5.26)$$

a result following from an argument analogous to that leading to (5.22).

Random walks, therefore, may have a highly non-trivial structure exhibiting fractal scaling. However, an unrestricted walk does not represent a real polymer chain appropriately, since it does not account for the repulsion between two molecules which are close together. In other words, a random walk can cross itself, while two monomers can not occupy the same position in space (excluded volume effect). The simplest modification to avoid this problem is to prohibit intersections: whenever a random walk would cross itself it is removed from the statistics. According to their definition *self-avoiding random walks* (SAW-s) do not grow indefinitely. They rather reproduce the equilibrium statistics of linear polymers in a good solvent. Since we are more interested in non-equilibrium, truly growing phenomena next we shall consider a never stopping version of SAW.

The following rules define a model called *true self-avoiding walks* (TSAW) (Amit *et al* 1983) already discussed in part in Example 4.1. The walker jumps at each time step to one of the neighbouring sites with a probability depending on the number of times the new site has been visited in the past. In particular, the probability  $p_{ij}$  of jumping from site  $i$  to the neighbouring site  $j$  is in the model equal to

$$p_{ij} = \frac{e^{-g_{ij} n_k}}{\sum_{k=1}^z e^{-g_{ik} n_k}}, \quad (5.27)$$

where  $g_{ij}$  is a parameter controlling the degree of inhibition associated with the particular bond  $ij$ ,  $n_k$  is the number of times the site  $k$  has been visited before and  $z$  is the lattice coordination number. The strongest inhibition is provided by the limit when all  $g_{ij} \rightarrow \infty$ , but TSAW can cross itself even in this limit. This occurs when there is no previously unvisited neighbour, and

is made possible by the normalization included in (5.27).

The upper critical dimension and the fractal dimension  $D = 1/\nu$  of TSAW have been investigated by various approaches. According to heuristic arguments (Pietronero 1983, Obukhov and Peliti 1983) one first assumes that the root mean square end-to-end distance  $R_0(t)$  is the only relevant length measuring the size of a self-similar TSAW. In this case we expect the density  $\rho(r, t)$  of points visited in a walk of duration  $t$  to have the form

$$\rho(r, t) \sim t R_0^{-d} f\left(\frac{r}{R_0}\right). \quad (5.28)$$

Furthermore, assuming as usual that  $R_0(t) \sim t^\nu$ , the increase of  $R_0(t)$  due to the prolongation of a walk for additional  $\Delta t$  steps is given by

$$\Delta R_0 = R_0(t + \Delta t) - R_0(t) \sim t^{\nu-1} \Delta t. \quad (5.29)$$

This increase is primarily due to the repulsion effects forcing the walk to expand. The magnitude of this effect is expected to be proportional to the gradient of  $\rho(r, t)$  calculated at a distance from the origin approximately equal to  $R_0$ . From (5.28) we have

$$\left.\frac{d\rho(r, t)}{dr}\right|_{r \sim R_0} \sim t R_0^{-d-1} f(1) \sim t^{1-(d+1)\nu}. \quad (5.30)$$

Comparison of (5.29) and (5.30) leads to

$$D = 1/\nu = \frac{d+2}{2}. \quad (5.31)$$

The above result does not hold above  $d = 2$ , because in this case the repulsion effects become negligible compared with the outward expansion of the walk due to ordinary diffusion. Therefore, allowing self-intersection even by taking into account long living memory does not change the upper critical dimension. However, in  $d = 1$  TSAW exhibits different scaling behaviour from ordinary random walks and has a mass scaling exponent close to that predicted by (5.31).



Finally, there is a model called growing self avoiding trail (GSAT) which seems to lead to a fractal dimension different from  $D = 2$  in  $d = 2$ , although it allows for self intersection (Lyklema 1985). This is a growing self avoiding walk during which the condition of avoiding sites is changed so as not to allow the walker to pass through the same bond twice. Such a process never terminates except at the origin, because on a lattice with an even coordination number there are either at least two free bonds leading out from a site or none. The origin is a special point, where the number of free bonds is always odd. Extensive Monte Carlo simulations indicate that  $D \simeq 1.87$  in two dimensions and the unrestricted random walk value  $D = 2$  is recovered only in  $d = 3$ . Therefore, GSAT has an upper critical dimension  $d = 3$  at which logarithmic corrections of the form

$$R_0(t) \sim At(\ln t)^\alpha \quad (5.32)$$

are expected to modify the asymptotic behaviour. The simulations confirmed the above expression.

#### 5.4.2. Growing self-avoiding walks

In this section strictly self-avoiding walks will be considered, i.e., the walk will not be allowed to have intersections. However, in contrast to the equilibrium version of SAW, the walk is designed in such a way that it tries to avoid itself whenever it is possible. There are two possibilities: depending on the particular model a walk can be trapped by itself or it is bound to grow indefinitely.

The interest in growing self-avoiding walks is motivated by a well known transition in the conformation of polymer chains as a function of temperature  $T$  (de Gennes 1979). At high temperatures the molecules behave as ordinary SAW with a fractal dimension  $D = \frac{4}{3}$  in  $d = 2$ . Lowering  $T$  results in a collapse of the chains at a temperature  $T_\theta$  due to an attractive two-body interaction. In this tricritical  $\theta$  point the fractal dimension of chains is  $D \simeq 1.75$  ( $d = 2$ ). At  $T = 0$  one has a completely space filling SAW

with a trivial dimension. As we shall see below, a never terminating self-avoiding walk is a good candidate to describe the geometry of long molecules at the  $\theta$  point.

The *growing self-avoiding walk* (GSAW) can be defined as a simple modification of TSAW with  $g \rightarrow \infty$  (Majid *et al* 1984, Lyklema and Kremer 1984). In the case of GSAW the walker chooses an unoccupied neighbouring site randomly, with a probability  $p = 1/n$ , where  $n$  is the number of free neighbours. If  $n = 0$ , the walk terminates; this property represents the main difference from TSAW. The scaling of  $R_0(t)$  with the number of steps  $t$  in principle could be studied by exact enumeration of the possible walk configurations (Section 4.3.). When calculating the average end-to end distance each configuration enters the sum by its own weight  $P_{t,i} = \prod_j p_{t,i}(j)$  which is the product of the probabilities  $p_{t,i}(j)$  of adding the  $j$ th new step to the  $i$ th configuration of length  $t$  (for ordinary SAW all  $P_{t,i}$ -s are equal). Knowing  $R_0(t)$  one can use expression (4.20) to estimate the fractal dimension. However, it turns out that in the case of GSAW the typical cluster size available in the exact enumeration approach ( $t \simeq 20$  steps) is not enough to see the true behaviour.

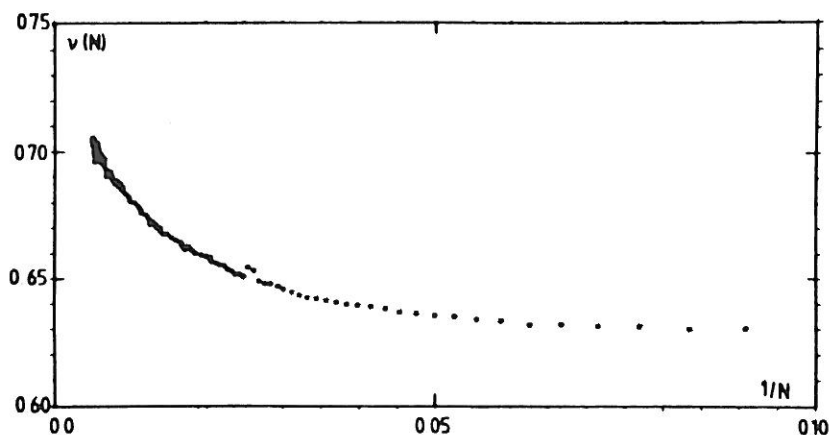


**Figure 5.6.** Extrapolation of the effective exponent  $\nu(t) = 1/D(t)$  obtained from high precision Monte Carlo simulations of growing self-avoiding walks up to a chain length of  $t = 200$  steps (Kremer and Lyklema 1985a).

To see the scaling of  $R_0$  one should carry out high precision Monte Carlo simulations up to sizes  $t \simeq 200$  (Kremer and Lyklema 1985a), and



this figure that when the walker approaches his previous path, in order to avoid trapping, he can use the knowledge of the local configuration and a quantity, called the winding number, attributed to the already visited sites. This number is equal to  $n_l - n_r$ , where  $n_l$  and  $n_r$  denote respectively the number of left and right turns made previously by the walker. In addition, Fig. 5.7 demonstrates the irreversibility of such walks which can be checked by simply calculating the corresponding jump probabilities for a reverse walk along the same path. In order to recognize whether a new possible step leads into a trap it is enough to consider all sites which form the smallest closed path in the forward direction. This means that for the triangular lattice only nearest neighbour (nn) sites, on the square lattice next to nn sites, while on the honeycomb lattice all next to next nn sites have to be examined together with the corresponding winding numbers.

An early numerical study based on exact enumeration of the configurations gives for the fractal dimension of IGSAW  $D \simeq 1.75$  (Kremer and Lyklema 1985b) indicating that IGSAW has different scaling behaviour from the previously considered models. Actually, the value

$$D = 1.75 = \frac{7}{4} \quad (5.33)$$

can be shown to be exact by establishing a correspondence between IGSAW and walks along the external perimeter or "hull" of an infinite percolation cluster (Weinrib and Trugman 1985). Then (5.33) follows from an exact result for the fractal dimension of the latter process (Saleur and Duplantier 1987).

First we show that the ring-forming version of IGSAW on a honeycomb lattice reproduces the perimeter of critical percolation clusters (Weinrib and Trugman 1985). The rules of this version of the original model are somewhat different: the origin is an allowed site, and a walk is considered to become trapped if it enters a region from which there is no path to the origin. However, one has good reasons to expect that the fractal dimension of large walks is the same in both versions. Honeycomb lattice is considered because for this lattice there is a one-to-one correspondence between the walk and the

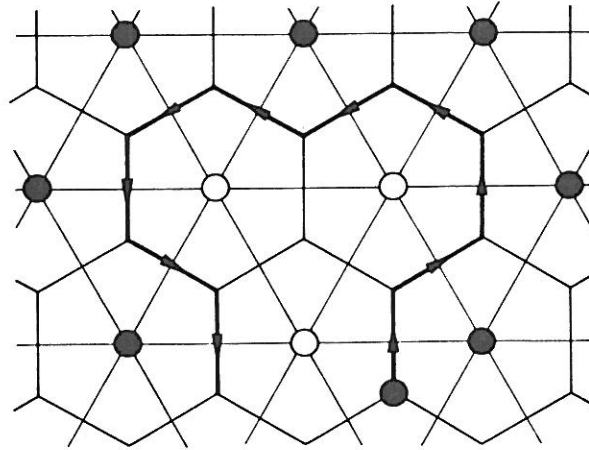


**Figure 5.8.** Example for a short IGSAW on the hexagonal lattice. It follows the perimeter of a site percolation cluster on the dual triangular lattice.

external perimeter of the site percolation clusters on a triangular lattice at its percolation threshold. (The equivalence is exact only for the ring-forming version.)

Consider the site percolation problem on the triangular lattice which is dual to the honeycomb lattice. The perimeter of a cluster can be defined as the bonds on the dual lattice separating filled from empty sites. Let us imagine that we build up the edge of a percolation cluster by deciding the occupation of a site determining the perimeter as we proceed. At each step one makes a decision whether a given site is occupied (with probability  $p_c = \frac{1}{2}$  or empty (with probability  $1 - p_c = \frac{1}{2}$ ). This choice determines whether the perimeter turns left or right at that step. Moreover, as demonstrated in Fig. 5.8, when the perimeter approaches itself the condition of self-avoidance is automatically satisfied, since the occupation of the corresponding sites has already been determined. The perimeter separates occupied from empty sites, thus it can not cross itself or enter a trap.

In this way IGSAW on a honeycomb lattice traces out the *hull of critical percolation clusters*. In this sense it is equivalent to an analogous walk designed with the purpose of generating the external perimeter of percolation clusters (Ziff *et al* 1984, Ziff 1986). On the basis of universality valid for the

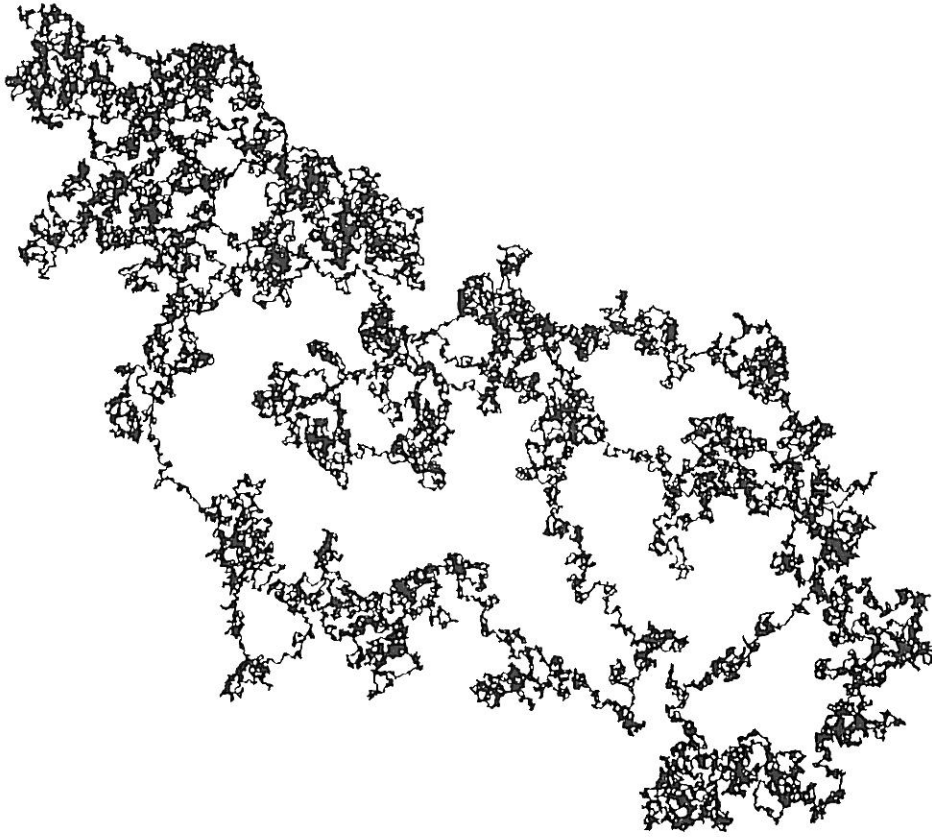


**Figure 5.9.** External perimeter of a percolation cluster generated by the ring-forming version of IGSAW on the square lattice. This configuration contains 194 468 sites (Ziff 1986).

critical behaviour of percolation the same statement can be extended to other types of two-dimensional lattices. A long perimeter walk on the square lattice is shown in Fig. 5.9. to demonstrate the structure of such walks.

The proof of (5.33) is completed by finding the fractal dimension of the hull. Assuming that the front of diffusing particles is equivalent to the perimeter of large percolation clusters, theoretical arguments (Saleur and Duplantier 1987) led to the following expression for the fractal dimension of the hull

$$D = 1 + 1/\nu_p = \frac{7}{4}, \quad (5.34)$$

where  $\nu_p = \frac{4}{3}$  is the correlation length exponent for percolation known exactly. An exact derivation of (5.34) can be obtained using the formulation

of percolation as a  $q = 1$  Potts model, and applying a Coulomb-gas mapping technique. Furthermore, it can be shown that hulls (i.e., IGSAW) are directly related to a SAW with short range attraction, thus they are expected to be in the same universality class as chains at the  $\theta$  point. IGSAW is also related to the front of diffusing particles in  $d = 2$  (Sapoval *et al* 1985). We conclude the description of IGSAW by mentioning that finding an algorithm for the  $d > 2$  case is far from trivial and no successful attempt has been published yet. The reason is that in  $d > 2$ , non-local information is required to avoid traps.

The last model discussed in this Section simulates linear aggregation. It generates a one parameter family of strictly self-avoiding, indefinitely growing walks. In this model the jump probability is determined by solving the Laplace equation with appropriate boundary conditions. One of the advantages of this *Laplacian random walk* (LRW) is that it can be defined in any dimension.

LRW grows according to the following rules (Lyklema and Evertsz 1986). Imagine a configuration centred at the middle of a circle having a radius much larger than the size of the walk. For this configuration the Laplace equation  $\nabla^2 \phi = 0$  is solved with a boundary condition  $\phi = 0$  on the walk and  $\phi = 1$  on the sphere. Let us define the probability of jumping to a given neighbouring site to be proportional to the potential at this possible new position. As a result the walk is self-avoiding and never stops, since the potential is zero in the cages (because of screening) and on the walk itself.

A simple generalization can be accomplished by choosing the probability of jumping to site  $i$  equal to

$$p_i = \frac{\phi_i^\eta}{\sum_j \phi_j^\eta}, \quad (5.35)$$

where  $\phi_i$  is the value of the field at site  $i$ ,  $\eta$  is a parameter and  $j$  runs over the nearest neighbours. The parameter  $\eta$  governs the probability difference among allowed directions. For  $\eta = 0$  IGSAW is recovered. In fact, this analogy provides a non-local method for growing of IGSAW-s in dimensions

larger than 2. For  $\eta > 0$  ( $\eta < 0$ ) the walk is self-repelling (self-attracting), and has a smaller (larger) fractal dimension than IGSAW. The case  $\eta = 1$  is analogous to a model based on linear aggregation of diffusing particles (Debierre and Turban 1986).

### 5.4.3. Walks on fractals

The problem of random walks on fractals has attracted great interest recently (for reviews see Aharony 1985, Havlin and Ben-Avraham 1987). Here we shall discuss only some of the specific aspects of this field which are related to fractal growth. The condition of self-avoidance will not be considered, thus we can refer to random walks on fractals as diffusion on a fractal substrate.

Consider the random motion of a particle placed onto a fractal network of dimension  $D$  made of bonds or filled sites. The walk starts at  $t = 0$  and the particle jumps with equal probability to any of the nearest neighbour sites belonging to the fractal. Its mean squared distance from the origin is expected to scale with the number of steps (time) as

$$R_0^2(t) \sim t^{2/d_w}, \quad (5.36)$$

where the exponent  $d_w$  depends on the structure of the fractal in a non-trivial way. For diffusion on Euclidian lattices  $d_w = 2$ . But the trajectory of a diffusing particle expands slower on a fractal, and in general  $d_w > 2$ .

Writing (5.36) in the form  $t \sim R_0^{d_w}$  suggests that  $d_w$  is a fractal dimension-like quantity. However,  $d_w$  is typically not the fractal dimension of the trail as a geometrical object, but describes the fractal scaling of mass (number of steps) within a region of radius  $R_0$ . While on Euclidian lattices the fraction of self-intersections becomes negligible in dimensions  $d > 2$ , in the case of fractal substrates returns to already visited sites play a relevant role in all  $d$ , except very special constructions. This is indicated by the fact that generally  $d_w > D$ . For example,  $d_w = \ln(d+3)/\ln 2 > \ln(d+1)/\ln 2 = D$  for the  $d$ -dimensional versions of Sierpinski gaskets (Havlin and Ben-Avraham 1987), or  $d_w = D + 1$  for the fractal shown in Fig. (2.1)



(Guyer 1985) when defined in  $d$  dimensions. Moreover,  $d_w$  can be larger than  $d$ . This is the case, i.e., for diffusion on percolation clusters up to  $d = 6$ .

The anomalous diffusion law represented by (5.36) can be supported by Monte Carlo simulations, scaling arguments or solutions of the problem for simple systems. The following derivation based on scaling arguments demonstrates that (5.36) is equivalent to the assumption (O'Shaughnessy and Procaccia 1986)

$$\sigma(r) \sim \sigma_0 r^{-\theta}, \quad (5.37)$$

with  $\sigma(r)$  defined through  $\sigma_{tot}(r) \sim \sigma(r)r^{D-1}$  which is the total conductivity (or diffusivity) of a shell of  $n(r) \sim r^{D-1}$  sites being at a distance  $r$  from the origin of walk. To see this let  $p(r, t)$  denote the average probability per site at time  $t$  of finding the particle within the shell between  $r$  and  $r + dr$ . Then the conservation of probability requires that

$$\frac{\partial}{\partial t} [(n(r)p(r, t))] = \frac{\partial}{\partial r} \left( n(r)\sigma(r) \frac{\partial p(r, t)}{\partial r} \right). \quad (5.38)$$

Inserting (5.37) and the expression for  $n(r)$  one obtains the diffusion equation in the form

$$\frac{\partial p(r, t)}{\partial t} \simeq \frac{1}{r^{D-1}} \frac{\partial}{\partial r} \left( \sigma_0 r^{D-1-\theta} \frac{\partial p(r, t)}{\partial r} \right) \quad (5.39)$$

which has the exact solution

$$p(r, t) = \text{Const } t^{-D/(2+\theta)} \exp \left\{ -\frac{r^{2+\theta}}{\sigma_0(2+\theta)^2 t} \right\}. \quad (5.40)$$

From (5.40) one can easily obtain the main quantities of interest. First, we see that (5.40) is equivalent to (5.36) with  $d_w = 2 + \theta$ , since

$$R_0^2(t) = \int_0^\infty r^2 n(r) p(r, t) dr \sim t^{2/(2+\theta)}. \quad (5.41)$$

Next we observe that  $N(t)$ , the total number of distinct sites visited scales with time as

$$N(t) \sim t^{D/(2+\theta)} = t^{d_s/2} \quad (5.42)$$

because  $p(0, t)$ , the probability of returning to the origin is inversely proportional to  $N(t)$ . In (5.42)

$$d_s = 2D/d_w \quad (5.43)$$

denotes the so called *spectral dimension*. This quantity enters the spectral density of vibrational modes of a fractal in the form of dimension, hence its name (Alexander and Orbach 1982).

Anomalous diffusion in inhomogeneous media has been extensively studied using percolation models (Gefen *et al* 1983). It was recognized that  $d_s$  is surprisingly close to  $\frac{4}{3}$  for percolation clusters in dimensions  $1 < d \leq 6$ . This fact led to a conjecture (Alexander and Orbach 1982) about the superuniversality of  $d_s$ , giving rise to a large number of controversial results about its validity for percolation. Scaling arguments can be used to express the spectral dimension for the infinite percolation network at the threshold through known standard exponents  $\beta$ ,  $\nu_p$  (see Section 5.1.) and  $\mu$ , where the conductivity scales as  $\sigma \sim (p - p_c)^\mu$ . The result is (Alexander and Orbach 1982)

$$d_s = 2 \frac{d\nu_p - \beta}{\mu - \beta + 2\nu_p}. \quad (5.44)$$

Finally, we discuss the fractal nature of growth sites which belong to the fractal and are nearest neighbours of the already visited sites (they are analogous to the live sites defined in Section 5.1.). Let us denote the number of growth sites at time  $t$  by  $G(t)$ . The following relation has been proposed between  $N(t)$  and  $G(t)$  (Rammal and Toulouse 1983)

$$\frac{dN(t)}{dt} \sim \frac{G(t)}{N(t)} \quad (5.45)$$

expressing the assumption that the probability of access to a growth site ( $dN/dt$ ) is proportional to the number of growth sites, and is inversely proportional to the number of already visited sites. Integrating (5.45) and using (5.36), (5.42) and (5.43) we have

$$G(t) \sim t^{2D/d_w - 1} \sim R_0(t)^{2D - d_w}, \quad (5.46)$$

where  $2D - d_w$  is the effective fractal dimension of the set of growth sites. This result is supported by simulations of diffusion on a Sierpinski gasket-type deterministic fractal (Havlin and Ben-Avraham 1987). Plotting  $\ln G(t)$  against  $\ln N(t)$  the slope of the straight line fitted to the data is  $x \simeq 0.53$  in good agreement with  $x = 2 - 2/d_s \simeq 0.535$  obtained from (5.46), where  $G(t) \sim N(t)^x$ .